Geol. Soc. Australia Spec. Publ. **22**, and *Geol. Soc. America Spec. Pap.* **372** (2003), 25–40

Surface-wave studies of the Australian region

E. DEBAYLE[1]* AND B. L. N. KENNETT[2]

[1] *IPGS — Ecole et Observatoire des Sciences de la Terre, CNRS and Université Louis Pasteur, 5 rue René Descartes, 67084 Strasbourg, France.*

[2] *Research School of Earth Sciences, Australian National University, ACT 0200, Australia.*

The deployment of portable stations over the Australian continent since the beginning of the 1990s has allowed the collection of a unique dataset for surface waves at regional distances. Surface wave tomographic inversions now exploit the excellent azimuthal ray coverage available for central and eastern Australia, so that S wave tomographic models for the upper mantle can be built with a lateral resolution of few hundred kilometres and a vertical resolution of a few tens of kilometres. Our tomographic models include an anisotropic component in addition to the distribution of S-wave heterogeneities. When only Rayleigh waves are considered in the inversion, this anisotropic component is represented at each depth in the mantle by the direction of fast horizontally propagating SV waves. When Love and Rayleigh waves are inverted simultaneously, the anisotropic component reflects the difference in wave speed between S waves polarised in horizontal and vertical directions. Our results for the simultaneous inversion of Love and Rayleigh waves agree with previous studies to locate the anisotropy in the uppermost 200–250 km of the mantle. However, there are significant differences between the different models deduced from the Rayleigh wave inversions. We show that the most likely cause of these differences is the frequency band used in the analysis of the seismograms. The application of path averages directly to shear-wave slowness is a reasonable assumption for the recovered models. The shear-wave speed models are found to be robust, especially when removing paths likely to have experienced a complex propagation. In the light of these new inquiries, we attempt to extract the well-resolved part of the surface-wave inversion and to see how far it can be reconciled with other results obtained from body-waves studies. It appears that, due to the horizontal smoothing imposed by surface waves and the difficulty of estimating the best choice for the frequency band used in analysis, the details of the anisotropic directions in the upper layer should be interpreted with caution. However, the existence of at least two layers of anisotropy is well constrained. In the upper layer, the complex anisotropy would reflect 'frozen' deformation in the lithosphere while in the lower layer the smoother pattern is more likely to reflect present-day deformation due to the northward motion of the Australian Plate. The observation that anisotropy is not vertically coherent with depth is more easy to reconcile with other anisotropic measurements inferred from body waves.

KEY WORDS: anisotropy, Australia, surface waves, tomography, upper mantle.

INTRODUCTION

The subduction zones to the north and east of Australia provide frequent events over a broad range of depths which can be exploited in surface-wave tomography of the Australian region. The mid-ocean ridge to the south of the continent provides a less frequent, but very useful, set of shallow events. There are only a limited number of permanent seismic stations with high-fidelity broadband recording in the region and these have been supplemented by extensive deployments of portable broadband instruments. The SKIPPY experiment (van der Hilst *et al.* 1994) occupied 60 sites across the continent in a series of deployments from 1993 to 1996 and subsequent experiments have improved coverage in southeastern Australia and different parts of Western Australia (Kennett 2003).

Fundamental and higher mode Rayleigh waves recorded on vertical component seismograms have been exploited in a number of tomographic studies of the shear-wave speed distribution beneath the Australian region. Zielhuis and van der Hilst (1996) analysed the data from the SKIPPY stations in eastern Australia using the Partitioned Waveform Inversion technique of Nolet (1990). They produced the first clear evidence of a substantial difference in the structure in the mantle beneath the Precambrian regions of the centre and west of the continent and beneath the Phanerozoic belt in the east. The path coverage was extended to nearly the whole continent by van der Hilst *et al.* (1998). This work revealed a consistent pattern of a mantle lithosphere extending to around 250 km depth beneath the shield regions, contrasted with a thinner lithosphere (about 100 km thick) below the eastern part of Australia, underlain by a significant low velocity zone for S waves.

Subsequently the number of available data have been augmented in various ways. Simons *et al.* (1999) have included data from the Australian Geological Survey Organisation stations and undertaken a study of regionalisation based on the geologic provinces in the continent. Debayle and Kennett (2000a) have exploited almost 2200 paths using an automated waveform analysis procedure (Debayle 1999) based on the work of Cara and Lévêque

* Corresponding author: Eric.Debayle@eost.u-strasbg.fr

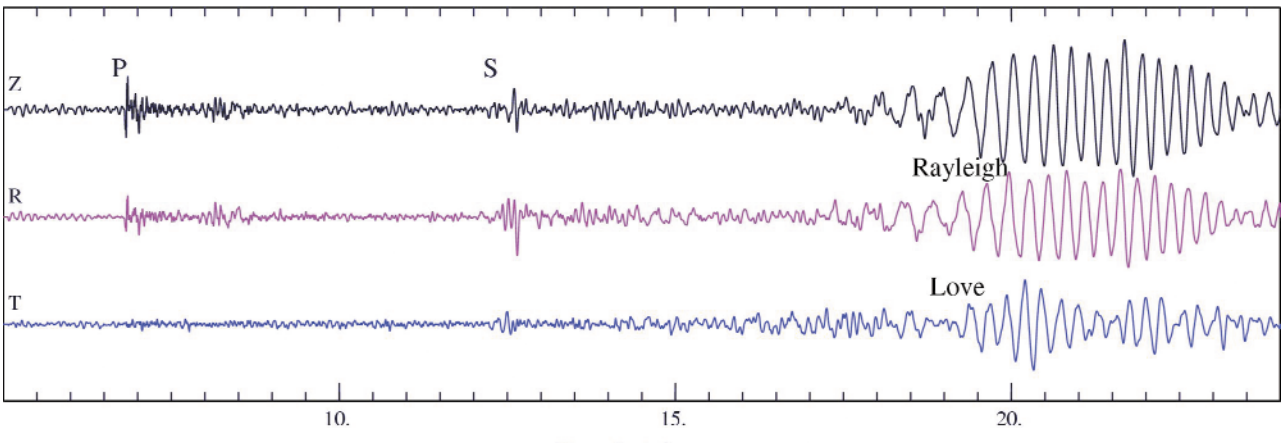

Figure 1 Unfiltered three-component seismograms at station SC08 in the Northern Territory for a shallow event near Tonga at 34°S, showing well-developed surface waves. The fundamental Rayleigh and Love modes constitute the prominent part of the surface waves for this shallow earthquake. Higher modes are less energetic and appear at the head of the surface wavetrain.

(1987), with a continuous regionalisation procedure for extracting a 3-D shear-wave speed model (Montagner 1986). In addition to the shear-wave speed distribution Debayle and Kennett (2000a) have examined the azimuthal anisotropy of the Rayleigh waves as a function of position and depth. Beneath the centre of the Australian continent there is a clear shift in the direction of fast polarisation from nearly east–west at 100 km to close to north–south at 200 km depth. The orientation at greater depth is roughly aligned with the direction of absolute plate motion.

Three-component recording of the seismic wavefield allows also the exploitation of horizontal component records. Debayle and Kennett (2000b) have undertaken simultaneous inversion of the Rayleigh and Love wave records from 792 event-station pairs. The two types of surface waves have different polarisation and sampling of the structure. By working with both it is possible to constrain the relation of the velocities of vertically and horizontally polarised S waves. The 'polarisation anisotropy' revealed by this work lies dominantly in the uppermost 200–250 km of the mantle beneath the central and western Precambrian cratons where the Rayleigh wave studies indicate high shear-wave speed, but significant 'polarisation anisotropy' is also found below eastern Australia, on the edge of the craton.

These recent studies indicate the important interaction between anisotropy and heterogeneity, which can have considerable significance for the geodynamic interpretation of the heterogeneity. Because there are some significant differences in the various models proposed for the Australian region, we present here an investigation of the sensitivity of the 3-D models of shear-wave speed, derived from Rayleigh waves, to the frequency content employed in the analysis. For this purpose, we have built a new SV wave tomographic model, by reprocessing all our Rayleigh waveforms in a different frequency band. We also check the robustness of our model, by removing a subset of the data related to paths with complex propagation, and the applicability of the path average hypothesis directly to the shear slowness. Finally, in the light of these new constraints, we provide a synthesis of the various constraints on anisotropy from the surface-wave studies and independent work on SKS splitting (Clitheroe & van der Hilst 1998; Girardin & Farra 1998; Ozalabey & Chen 1999).

SURFACE-WAVE TOMOGRAPHY

For earthquakes at depths less than 100 km the surface waves normally form the most prominent part of a seismogram, as illustrated in Figure 1 for a shallow event in the Tonga region recorded in the Northern Territory. The horizontal component seismograms have been rotated to produce traces along the great circle to the source (R) and transverse to the path (T).

The Rayleigh waves with polarisation in a vertical plane appear on the vertical (Z) and radial (R) components, while the horizontally polarised Love waves arrive on the tangential (T) component. For a shallow event, as in Figure 1, the records are dominated by the fundamental mode surface waves, but for deeper sources there is also significant excitation of higher mode surface waves which have greater penetration into the Earth. The apparent frequency of the surface waves changes along the wavetrain, this dispersion arises because the waves have an interaction with the structure which depends on frequency. At high frequencies the surface waves are confined close to the surface, but at lower frequencies they penetrate to greater depth and are influenced by the higher seismic-wave speeds at depth. The effect of a change in shear-wave speed structure at a given depth on the fundamental and first four higher Rayleigh modes displacement field associated with Rayleigh waves is illustrated in Figure 2 for different periods. The fundamental mode decays fairly rapidly with depth but the higher modes show significant sensitivity to shear-wave structure in the transition zone.

By working with the fundamental and higher modes we have a probe into the Earth in which the character of the wavetrains is dictated by the structures encountered in the outer layers of the Earth and where the dependence on frequency provides information over a range of depths. In a

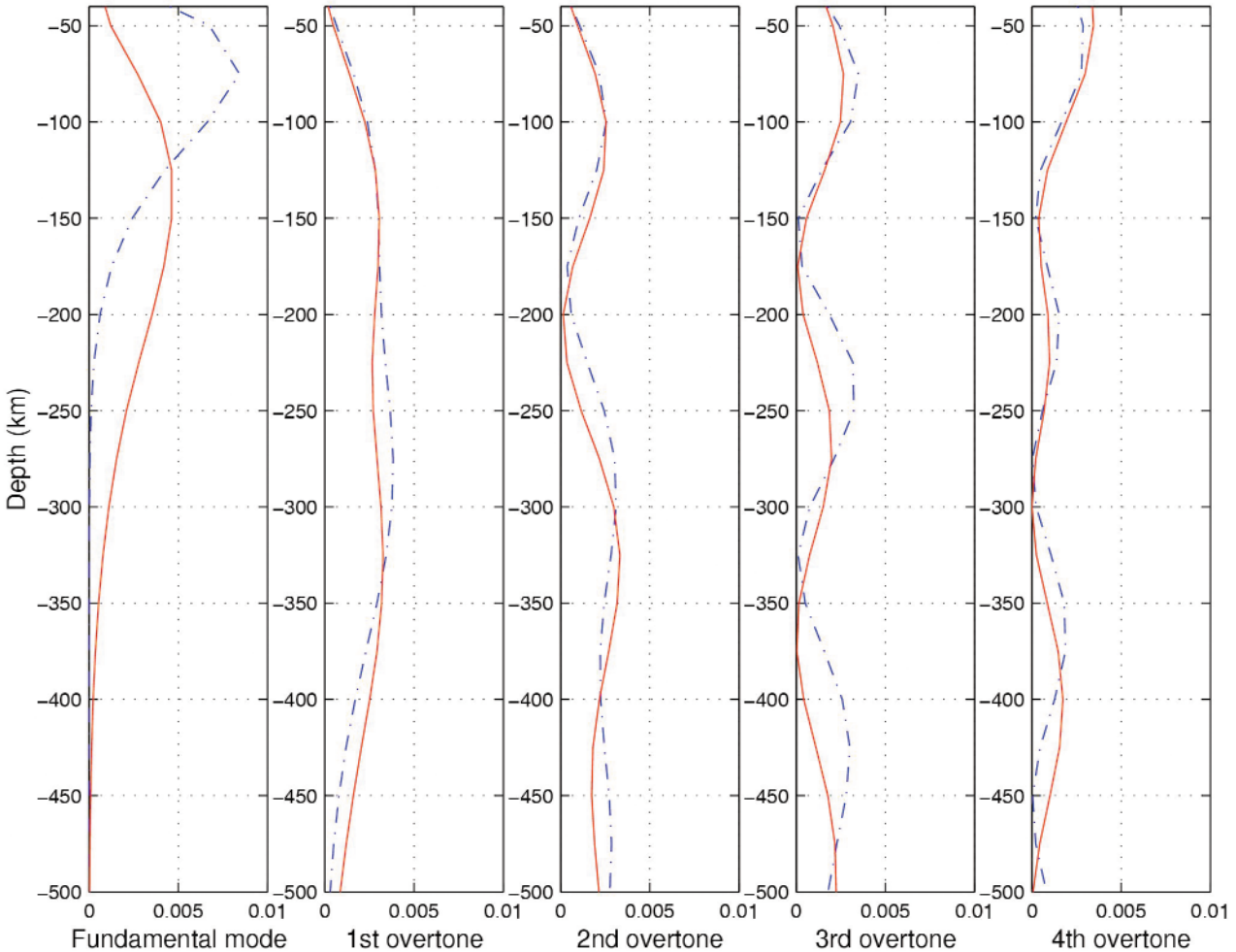

Figure 2 Sensitivity kernels for the fundamental and first four higher modes of Rayleigh waves at periods of 50 s (dash-dot line) and 160 s for the fundamental mode, and 50 s (dash-dot line) and 80 s for the higher modes (continuous line). The curves represent the relative partial derivatives of the phase velocity according to the shear-wave velocity $[(V_{sv}/C).(\partial C/\partial V_{sv})]$. These partial derivatives are shown for a 1 km thick layer.

smoothly varying medium the phase contribution for an individual mode represents an average of the phase slownesses encountered along the propagation path. This is the property which is exploited in surface-wave tomography.

When observations are available from a large number of paths crossing a region, the path-specific models can be combined to produce a 3-D image of shear-wave structure. The most effective means of extracting multimode information is to match the waveforms of observed and calculated seismograms based on a model of the source process. We employ the method of Cara and Lévêque (1987) which is able to achieve good results for the recovery of shear-wave speed profiles for significant deviations from a reference model (up to ±10% perturbations). The broad range of application is achieved by working with secondary variables based on the correlation of full seismograms with individual modal contributions. These secondary variables have a close to linear dependence on the perturbations in shear-wave speed from the reference model.

In order to achieve an effective application of the waveform inversion procedure, we have to ensure that we treat the portion of the seismogram that conforms to the underlying assumptions of independent mode propagation and that the receivers lie in the far-field of the source. Kennett (1995) has examined the nature of these approximations in laterally varying media. For paths longer than 2000 km, typical of the ranges used in this study of the Australian region, the fundamental mode should be useable in the period range from 160 to 40 s and the higher modes from 100 to 25 s period. At higher frequencies the modal contributions become susceptible to the influence of strong heterogeneity at shallow depth, and the propagation paths can deviate significantly from the great circle. When there are sharp variations in seismic properties in the mantle itself the assumption of smoothness, which is employed in the representation of the seismograms, may be violated and we then need to be cautious in the interpretation of the results.

The shear-wave speed models derived from the inversion of the waveforms of the surface wavetrains can be regarded as a summary of the multimode dispersion characteristics for the individual paths. When the deviations of the true 3-D model from the reference model are not too large, it is a reasonable approximation to transfer the path-average property of phase to the shear slowness. Under this assumption, the set of 1-D path-specific models derived from the waveform inversion can be regarded as linear constraints on the

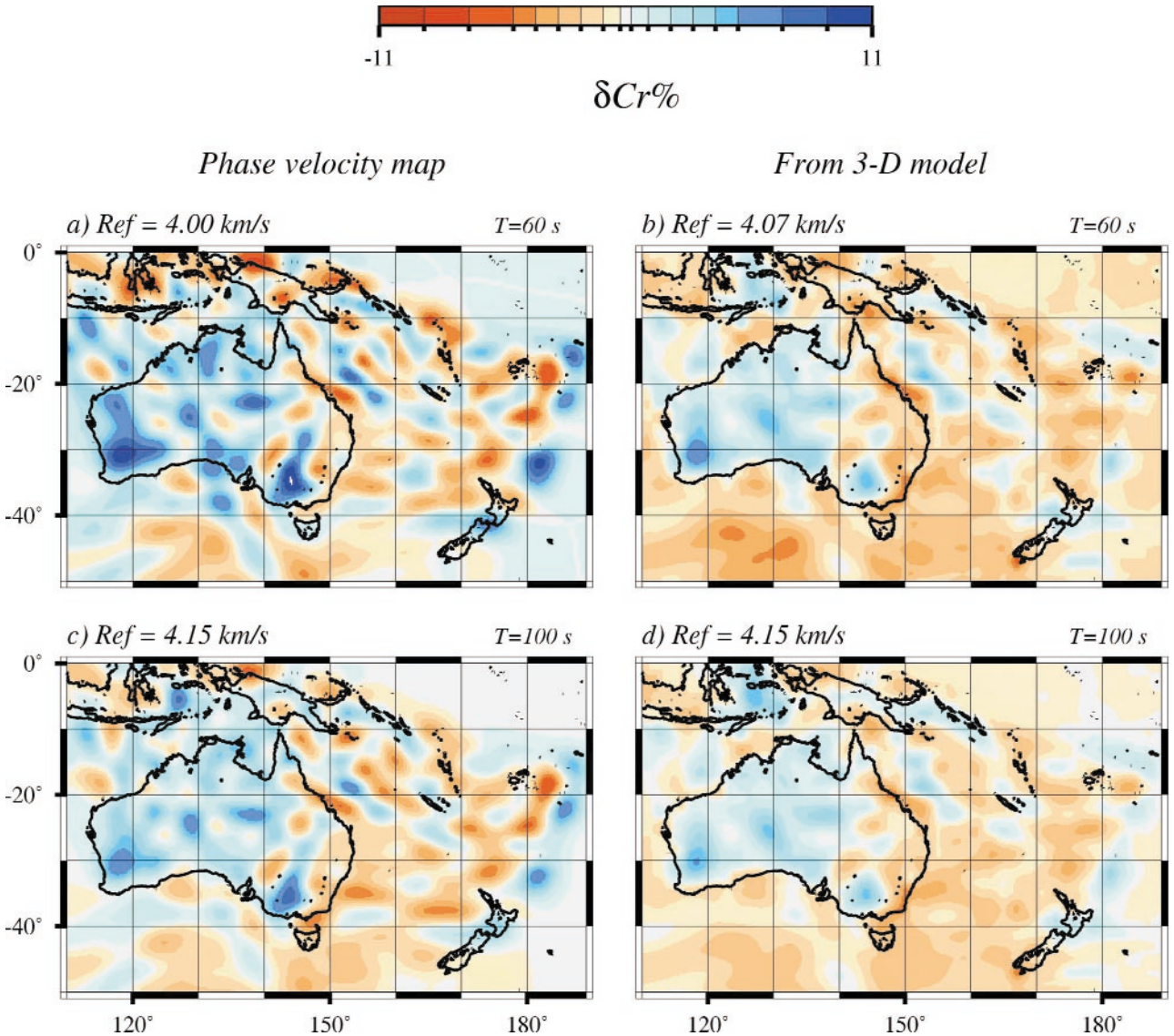

Figure 3 Phase velocity maps for Rayleigh waves at 60 and 100 s periods. (a, c) Obtained by applying the phase-velocity distribution directly to the phase slowness. (b, d) Predicted from the 3-D SV velocity model of Debayle and Kennett (2000a).

3-D shear-wave speed variations and a linear inverse problem can be posed for the recovery of the 3-D model. This is the approach employed by Debayle and Kennett (2000a, b).

However, where there are large contrasts in seismic-wave speeds, the path-average interpretation of the shear-wave speed models may not be adequate (Kennett & Yoshizawa 2002). In this case it is necessary to work through the intermediary of multimode phase slowness maps as a function of frequency, employing the path-average property of phase directly. The 3-D shear-wave speed can then be recovered from local inversions of the dispersion properties. In the following section, we test the validity of the path-average approximation directly to shear slowness, for the level of heterogeneity expected in Australia.

A TEST OF THE PATH-AVERAGE APPROXIMATION

The development of a 3-D wave-speed model in a two-stage process requires that the contrasts in seismic-wave speeds are not too large. This restriction is required to make the identification of the path-specific 1-D models as the average of the shear slowness along the path.

Kennett and Yoshizawa (2002) have pointed out that the 1-D model derived for a path is best regarded as a summary of multimode dispersion and that this interpretation can be employed even when the shear-slowness profile cannot be regarded as a path average. Since the contrasts in our models are quite large we need to examine the influence of the assumptions we have made in the shear-wave speed inversion. We can do this by comparing the predicted phase-velocity distribution derived from the 3-D model and a phase-velocity map produced by applying the path-average approximation directly to phase slowness, as in the original development of Woodhouse (1974).

We have used the results of Debayle and Kennett (2000a) using waves up to 40 s period and combine the phase-velocity information at 60 s and 100 s for the 2194 paths. The inversions for the 3-D wave-speed model and for the geographic distribution of phase speed have been car-

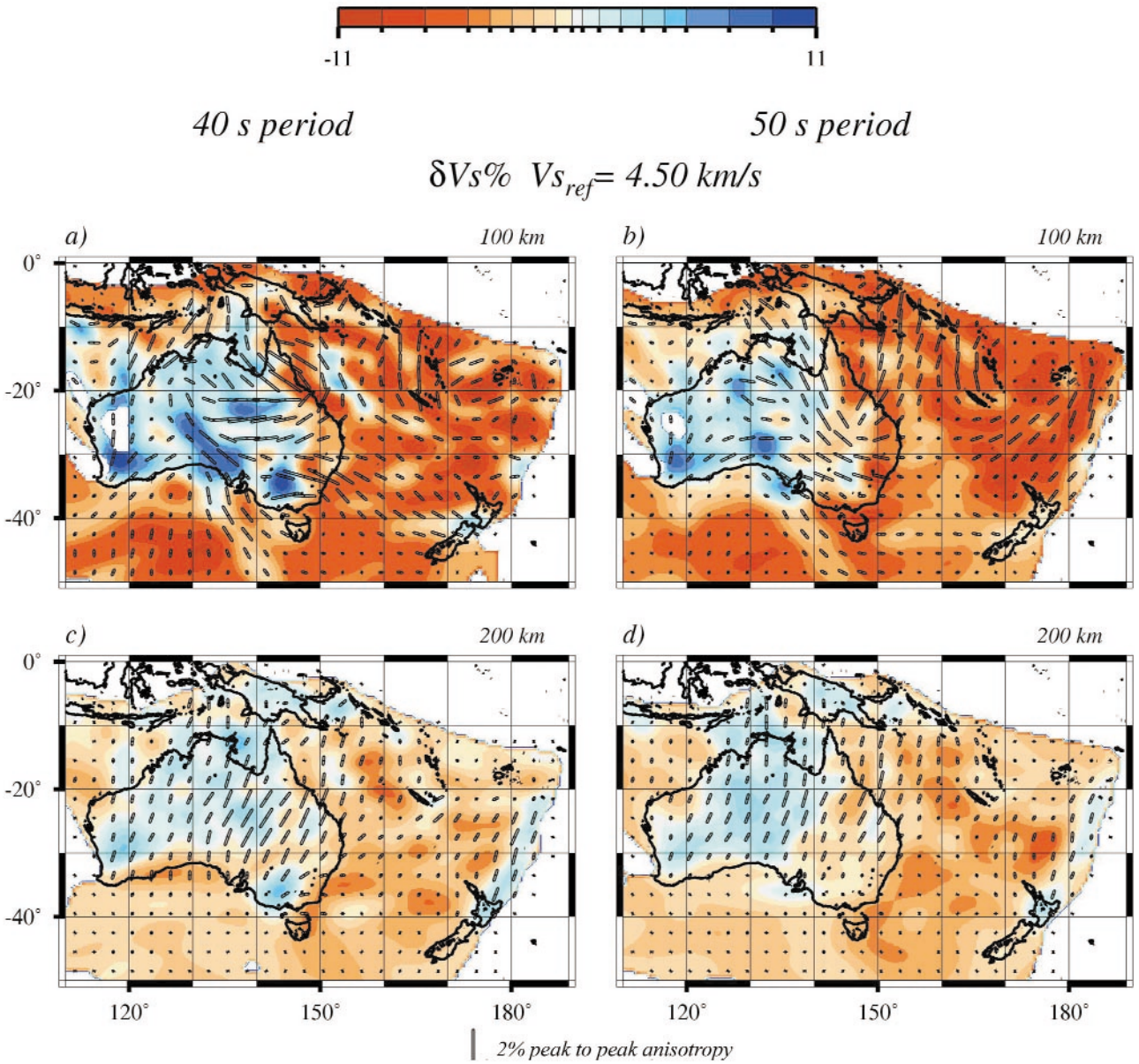

Figure 4 (a, c) SV wave heterogeneities and azimuthal anisotropy for an inversion with waveforms analysed for the frequency range 40–160 s. (b, d) Inversion for the frequency band 50–160 s. Tones represent velocity contrasts and bars display azimuthal anisotropy, the length of the bars indicating the strength of anisotropy.

ried out with the same continuous regionalisation technique, with the same assumed Gaussian spread about each path (with width 200 km) representing the model covariance. The agreement between the direct phase-velocity maps and those reconstructed from the 3-D shear-wave speed is good (Figure 3) with a very similar configuration of heterogeneity, although there are some slightly larger contrasts in the direct phase-speed maps. We note that for the upper layers of the model, some offsets in reference velocities are needed to bring the images into the closest correspondence. We believe that this is a symptom of a slight bias towards higher wave speeds in the 3-D model arising from the limitations of the two-step inversion.

The comparison of the direct calculations of the phase-velocity maps and those reconstructed from the model is very encouraging. We note though that the use of the phase average along each path rests on the assumption of smooth variations in wave speed on a scale long compared with the wavelength. The level of variation seen in the phase velocity maps in Figure 3a is such that we are at the limit of this assumption. For the fundamental mode at 100 s period, the wavelength in the mantle is around 420 km and is approaching the scale of the medium wavelength heterogeneity.

To extract any more information from the seismograms we will need to adopt a description of the propagation process with a full allowance for 3-D effects, including mode-coupling and refraction. The theoretical treatment of Kennett (1998) indicates how this can be accomplished, but is too computationally intensive for use with any current inversion schemes. Suitable restricted approximations need to be found to allow effective waveform modelling for the propagation of surface waves in 3-D heterogeneous models.

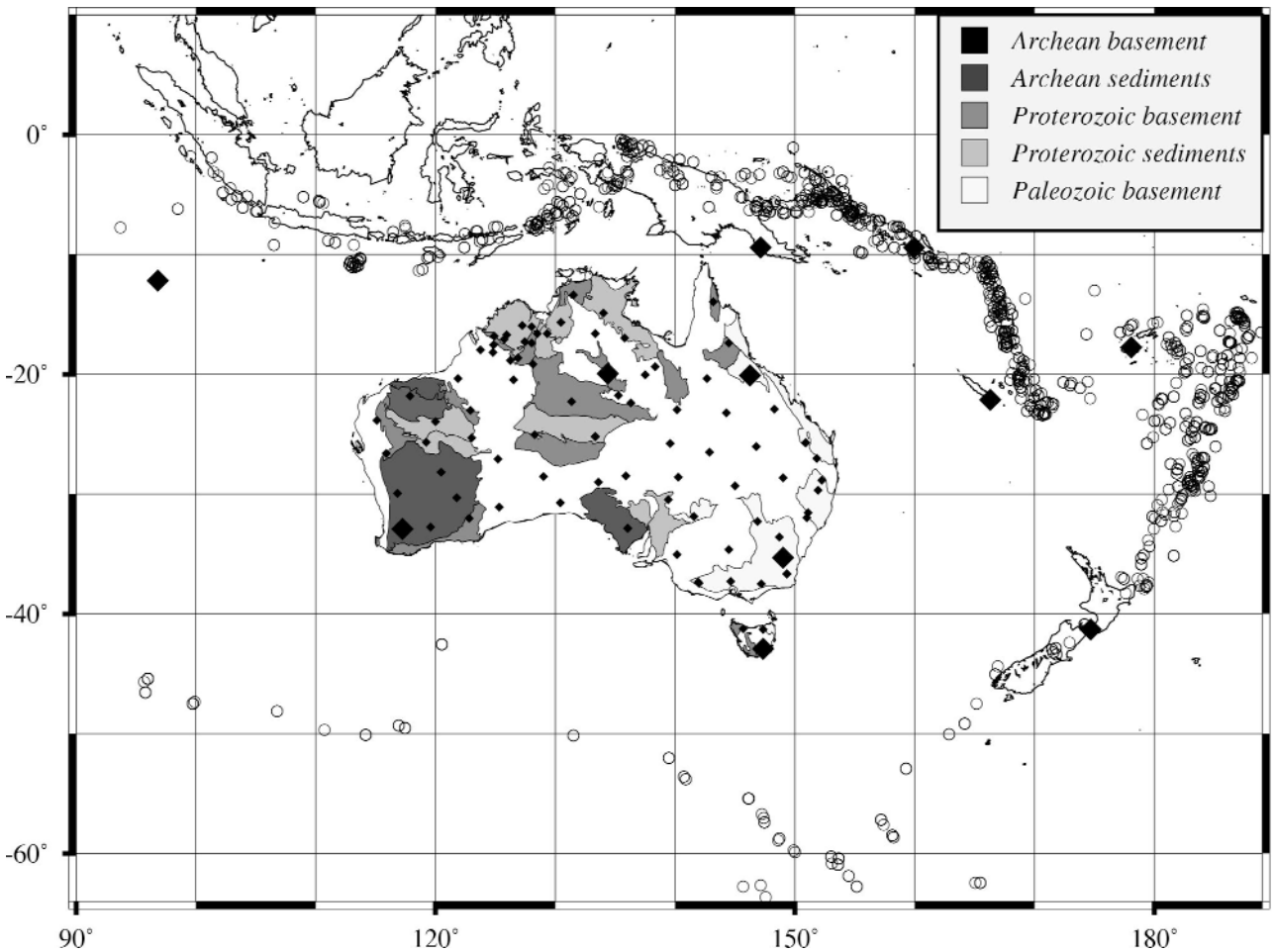

Figure 5 Location of events and stations used in the Rayleigh wave studies presented in this paper. The large diamonds indicate permanent stations from the IRIS and GEOSCOPE networks, whilst the smaller diamonds are the locations of portable broadband stations. Events are represented by open circles. The main geological outcrop zones are indicated in the background.

SV WAVE AZIMUTHAL ANISOTROPY FROM RAYLEIGH WAVE INVERSION

For Australia, even with the substantial level of heterogeneity present in the region, the application of path-averaging directly to shear-wave slowness is not likely to be a significant limitation if we restrict attention to periods between 160 and 40 s. We can therefore restrict our tomographic approach to a two-step process. In the first step, a waveform analysis provides path-average constraints on the shear-wave speed structure. In the second step, once path-average constraints have been obtained for a large number of paths with different azimuths, it is possible to extract from the tomographic inversion the SV wave anisotropic directions in addition to the shear-wave speed heterogeneities. The tomographic inversion is based on the work by Smith and Dahlen (1973) who demonstrated the azimuthal dependence of Rayleigh wave phase and group velocities in a slightly anisotropic medium. Providing the anisotropy is weak, such ordinary perturbation methods are justified for the period range used in the analysis, where the intrinsic coupling between Love and Rayleigh waves is expected to be weak (Maupin 1989). Montagner and Nataf (1986) then showed that the phase and group velocity azimuthal terms can be inverted for some combinations of the elastic coefficients at depth. For waveform fitting, which provides a direct estimate of 1-D path average SV wave models, the procedure needed to retrieve the distribution of heterogeneities and anisotropy at depth is described in detail by Lévêque *et al.* (1998). In particular, these authors showed that in a long period approximation in a full but weakly anisotropic medium, the path-average SV velocity models depend on the combination of elastic parameters best resolved by Rayleigh waves, which control the velocity of SV waves propagating horizontally at azimuth θ. The anisotropic directions presented in Figures 4, 7, 9 and 10 can be interpreted as the directions of fast SV wave propagation. Assuming that the main cause of anisotropy in upper mantle materials is the preferred orientation of olivine crystals, these anisotropic directions would point toward the projection of the fast a-axis of the crystals on the horizontal plane.

To investigate possible effects due to the frequency filtering of the seismograms, we present in Figure 4 the results of two inversions where waveform analysis has been performed in different frequency bands. Compared to the previous work by Debayle and Kennett (2000a), we use a more restrictive geographical distribution of events. We use only earthquakes that originate within the Indo-Australian Plate or along its major boundaries. We exclude events from the

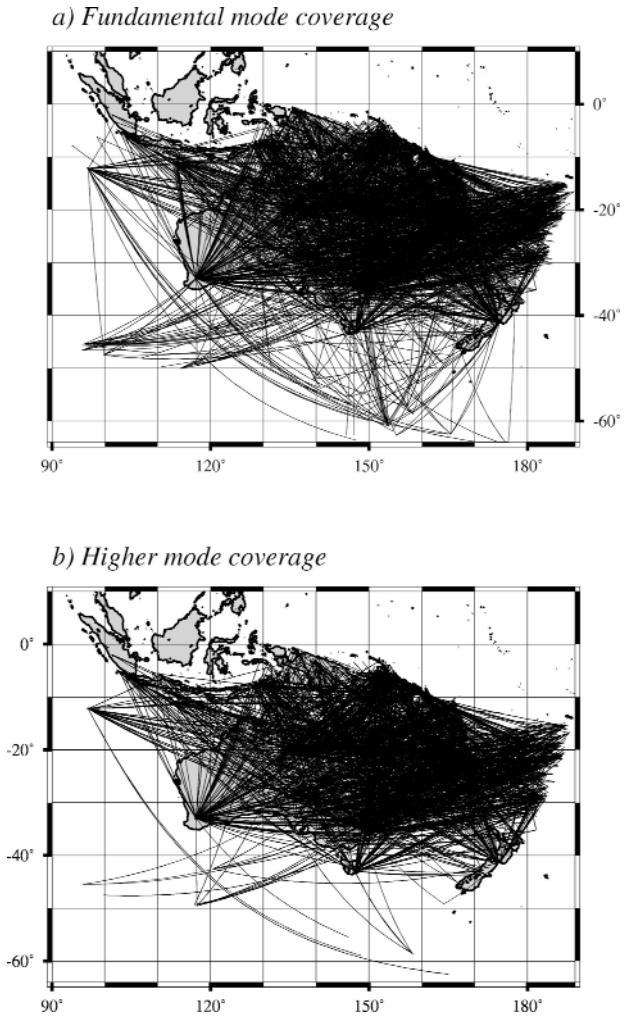

Figure 6 Path coverage for Rayleigh waves. (a) Data for which the fundamental modes have been taken into account in the inversion. (b) Data for which the higher modes have been taken into account.

trenches bounding the Philippine Sea that were previously used by Debayle and Kennett (2000a). This allows us to estimate the possible bias that may have been introduced previously by paths related to events with more complex source mechanisms or crossing complex structures such as the northern subduction zones.

Two maps (Figure 4a, c) have been obtained from an inversion in the period range 40–160 s, similar to Debayle and Kennett (2000a) using the same process of automated analysis of the individual paths, but with the removal of events in the vicinity of the Philippine Sea. Of the 2194 paths analysed by these authors, 1820 were retained. The distribution of events is shown in Figure 5 while the corresponding ray coverage in fundamental and higher modes is presented in Figure 6. The tomographic images obtained are very close to those presented by Debayle and Kennett (2000a) and demonstrate that no significant bias is introduced by paths coming from the Philippine Sea region.

Two maps (Figure 4b, d) have been obtained by reprocessing all the waveforms in the period range 50–160 s instead of 40–160 s. A total of 2482 waveforms were successfully matched with the automated process of Debayle (1999) and again whether or not we included paths related to events in the vicinity of the Philippine Sea did not affect the results.

Significant differences are observed in the uppermost layers, especially near 100 km depth, between the two inversion at 40 s and 50 s. These differences are more pronounced for short-wavelength heterogeneities, the long-wavelength component of the S wave structure being better preserved. For layers above 150 km depth, the choice of the cut-off period has a direct effect on the wave-speed model from the inversion because the S wave structure is mostly constrained by the fundamental Rayleigh mode between 40 and 100 s period (Figure 2). At greater depths, where 40 and 50 s period fundamental Rayleigh waves have low sensitivity, the differences between the wave-speed distributions for the two inversions diminish, and there is a good agreement between the two maps at 200 km depth (Figure 4c, d).

To explain the differences observed near 100 km depth (Figure 4a, b), several effects can be invoked. First, the horizontal resolution of our dataset increases when shorter periods are included in the inversion and it is likely that part of the observed difference between the 40 s and 50 s inversion reflects an actual difference in resolution. However, effects due to the crustal structure or produced by possible off-great-circle propagation are likely to be more important at shorter periods. Therefore, they may contribute to part of the difference observed between the 40 s and the 50 s inversion.

Crustal effects probably do not contribute significantly to the observed differences. Both inversions are performed using the same 3SMAC crustal structure (Nataf & Ricard 1995), which has an average crustal thickness of about 40 km for Australia. The maximum sensitivity of the Rayleigh waves at 40 and 50 s period is located below the crust at around 50 and 75 km depth, which indicates that in both cases we use a dataset primarily sensitive to the upper mantle.

For the fundamental mode near 40 s period, which provides strong constraints on the shallow structure of the model, the great-circle approximation should still be just valid for epicentre–station distances typical of this study (Kennett 1995). However, ray tracing in our tomographic model (Yoshizawa & Kennett 2002) shows that the strong gradient in shear velocity near the edge of the craton can produce significant deviations from the great circle at 40 s period for the fundamental and even the first higher mode. Debayle and Kennett (2000a) noticed that the strongest effects are expected to be associated with north–south paths grazing the continent edge, but this combination of source–receiver pairs was not actually present in the dataset used in their inversion. However, the differences observed at 100 km depth near the edge of the craton in Figure 4 suggest that off-great-circle effects at 40 s periods may contribute to bias in the 40 s inversion in this part of the model. We also note that even when great-circle deviations remain small at 40 s period, they increase rapidly when the period decreases and by 20 s period become important for the first few higher modes.

It is thus rather difficult to estimate which part of the differences in the 3-D shear-wave speed models presented in

Figure 4 should be attributed to a real difference in resolution or to the limitation in our approximations to the nature of the surface-wave propagation processes. We believe that the differences obtained with the inversions with upper limits of 40 and 50 s period reflect the level of confidence we should give to this class of tomographic inversion. Even if

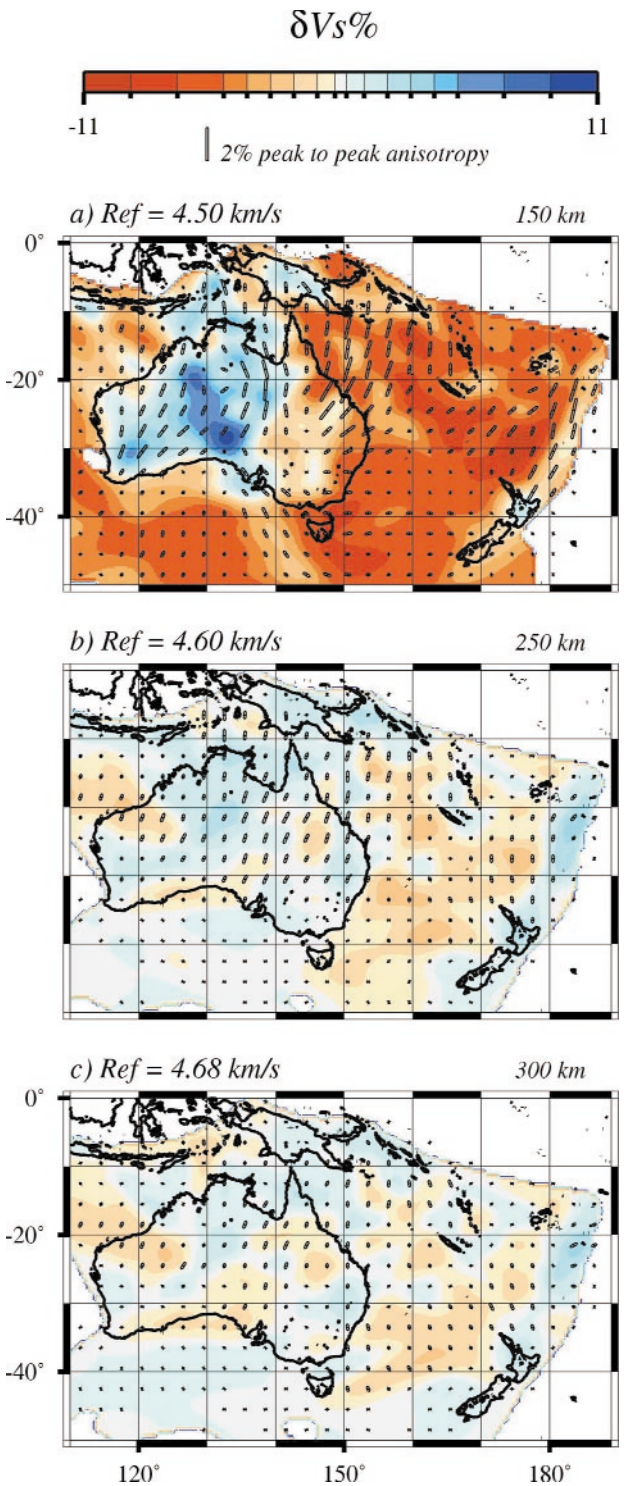

Figure 7 Slices at 150, 250 and 300 km depth in the SV velocity model from the Rayleigh wave inversion in the period range 50–160 s. As in Figure 4, tones represent velocity contrasts and bars display azimuthal anisotropy.

variations in seismic heterogeneities and anisotropy with wavelength smaller than 500 km should be interpreted with caution, the major changes are well constrained and provide useful indications of the deep structure of the Australian Plate.

Indeed, whether or not the inversion is pushed to include analysis at 40 s period, the main features of our tomographic inversions persist. As revealed in the previous inversion by Debayle and Kennett (2000a), a clear change in the organisation of seismic anisotropy occurs between the uppermost 100 km of the mantle and the deeper structure.

For the uppermost layer, down to 150 km depth, Figure 4 suggests that we should be cautious when interpreting the details of the complex anisotropic pattern. This is supported by a synthetic experiment where we tried to retrieve a complex pattern of anisotropy with 90° changes in anisotropic directions superimposed to the 3SMAC model (Figure 9): although the general anisotropic pattern is well retrieved east of 125°E, smoothing effects can locally lead to wrong anisotropic estimations in the vicinity of abrupt changes in anisotropic directions.

For the lowermost layer, below 150 km depth, a smoother pattern of anisotropy is retrieved for both the inversions (with either a 40 s or 50 s period upper bound). This confirms that present-day shearing occurs at the bottom of the Australian mechanical lithosphere, but still within the zone of elevated shear-wave speeds.

Finally, comparing our results with those previously obtained by van der Hilst *et al.* (1998) and Simons *et al.* (1999), we find a better agreement in the uppermost 200 km, between the results of our 50 s inversion and their published models. However, at depths greater than 200 km (Figures 7, 8), where the structure is mostly constrained by the higher modes, significant differences persist. The main differences from the models presented by van der Hilst *et al.* (1998) and more recently by Simons *et al.* (1999) may therefore be related to the treatment of higher mode information. In their use of the partitioned waveform inversion method (Nolet 1990; Zielhuis & Nolet 1994), van der Hilst *et al.* (1998) and Simons *et al.* (1999) push the higher mode analysis to periods up to 20 s. At 20 s period, off-great-circle effects become important and the size of the wavespeed variations suggest that mode coupling may need to be taken into account [cf. Marquering *et al.* (1996) in a study of structure in Europe].

LOVE/RAYLEIGH SIMULTANEOUS INVERSION

Rayleigh waves can be used to extract anisotropic directions efficiently because their azimuthal variation depends mostly on terms depending on $\cos 2\theta$, $\sin 2\theta$, where θ is the azimuth of the path. These dependencies can be recovered from a relatively modest number of crossing paths. In a cell defined by the horizontal resolution of the tomographic model, a minimum of three paths with different azimuths is necessary to recover the 2θ variation. However, with Rayleigh waves alone, it is often difficult to demonstrate the presence of anisotropy without ambiguity. This is because the azimuthal variation of Rayleigh waves generally contributes to explain only a small part of the misfit between

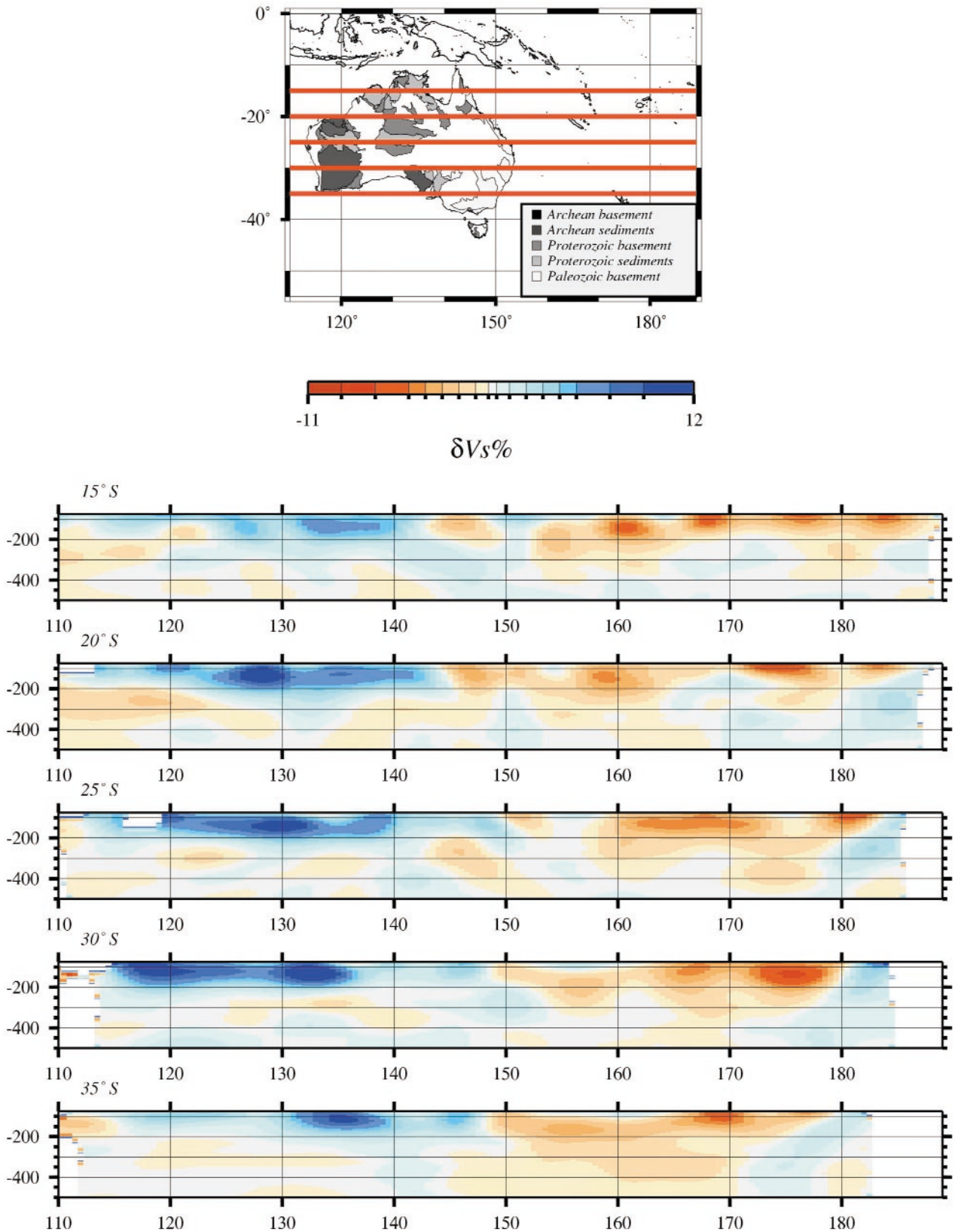

Figure 8 Vertical cross sections at different latitudes in the SV velocity model after the Rayleigh wave inversion in the period range 50–160 s.

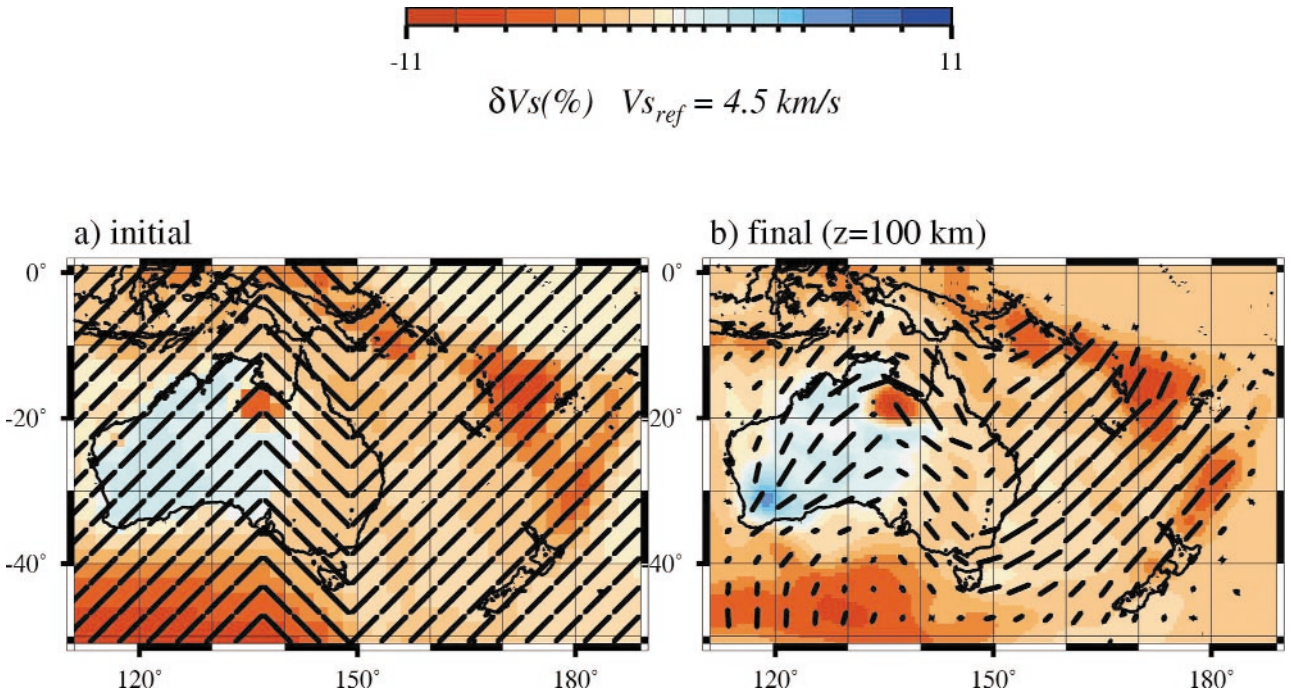

Figure 9 Synthetic experiment. (a) The initial model is the isotropic shear velocity distribution at 50 km depth provided by the 3SMAC model of Nataf & Ricard (1995) with a pattern of azimuthal anisotropy superimposed. (b) The result of the synthetic inversion is shown at 100 km depth.

observed and predicted seismograms. Many isotropic shear-velocity models have been found to give a satisfactory fit to Rayleigh waves, which suggests that in most situations it would be acceptable to suppress the azimuthal anisotropy.

A simultaneous inversion of the horizontal and vertical components of the surface wavefield is able to provide additional constraints on the presence, relative amplitude and depth location of seismic anisotropy. It is often difficult to explain the dispersion of both Love and Rayleigh waves with a single isotropic model (McEvilly 1964). Generally, the dispersion of the two classes of waves can be reconciled by adding a single anisotropic parameter which allows SH and SV waves to propagate at different velocities. The need to introduce this 'polarisation' or 'radial' anisotropy to reconcile the Love and Rayleigh wave components is considered as strong support for the presence of anisotropy in the upper mantle.

For the upper mantle beneath Australia, surface-wave polarisation anisotropy studies have been conducted by Gaherty and Jordan (1995) and Debayle and Kennett (2000b). Gaherty and Jordan (1995) used body and surface waves to build a depth-dependent 1D elastic model along a single corridor crossing Precambrian Australia. Their inversion revealed the presence of significant polarisation anisotropy down to 250 km in the upper mantle. Debayle and Kennett (2000b) chose a different strategy. They applied the automated procedure developed by Debayle (1999) for the simultaneous analysis of both Love and Rayleigh waves and analysed a larger dataset related to paths crisscrossing the Australian continent. A total of 792 pairs of Rayleigh and Love wave seismograms was used to retrieve the distribution of SV and SH velocity in the upper mantle. Each Love and Rayleigh pair is related to a single epicentre–station path and inverted for a radially anisotropic model compatible with the waveforms of both Love and Rayleigh waves. 1584 waveforms are used in the inversion. The number of paths is reduced compared to the Rayleigh-only inversion because the Love wave records are generally noisier.

We present in Figure 10 three slices through the SH and SV velocity distribution found by Debayle and Kennett (2000b). For SV waves, the cos 2θ, sin 2θ azimuthal variation could be recovered by constraining the horizontal smoothness of the model using Gaussian functions with correlation lengths of 500 km. This large horizontal degree of smoothing provides a smoother model compared to the Rayleigh-only inversion but confirms the presence of two anisotropic layers, the lower layer presenting a nearly north–south component in good agreement with the present-day motion of the Australian Plate. The upper layer is a smooth image of the Rayleigh-only inversion at 100 km depth, where east–west anisotropic directions dominate in central Australia.

For SH waves, the azimuthal variation is faster and dominated by terms in cos 4θ, sin 4θ which could not be recovered with the available Love/Rayleigh coverage, and Debayle and Kennett (2000b) preferred to average out the SH azimuthal variation by using the same horizontal degree of smoothing in the inversion as for the SV waves, so that the maps could be compared.

Figure 10 shows that the SV and SH heterogeneity patterns are relatively close if an increase of about 4% is used for the SH reference velocity in the uppermost 200 km of the mantle. On average, the amplitude of the SH/SV difference would be about 4–5% but locally there are larger differences. This can be seen in Figure 11 where the parameter ξ which represents the radial anisotropy

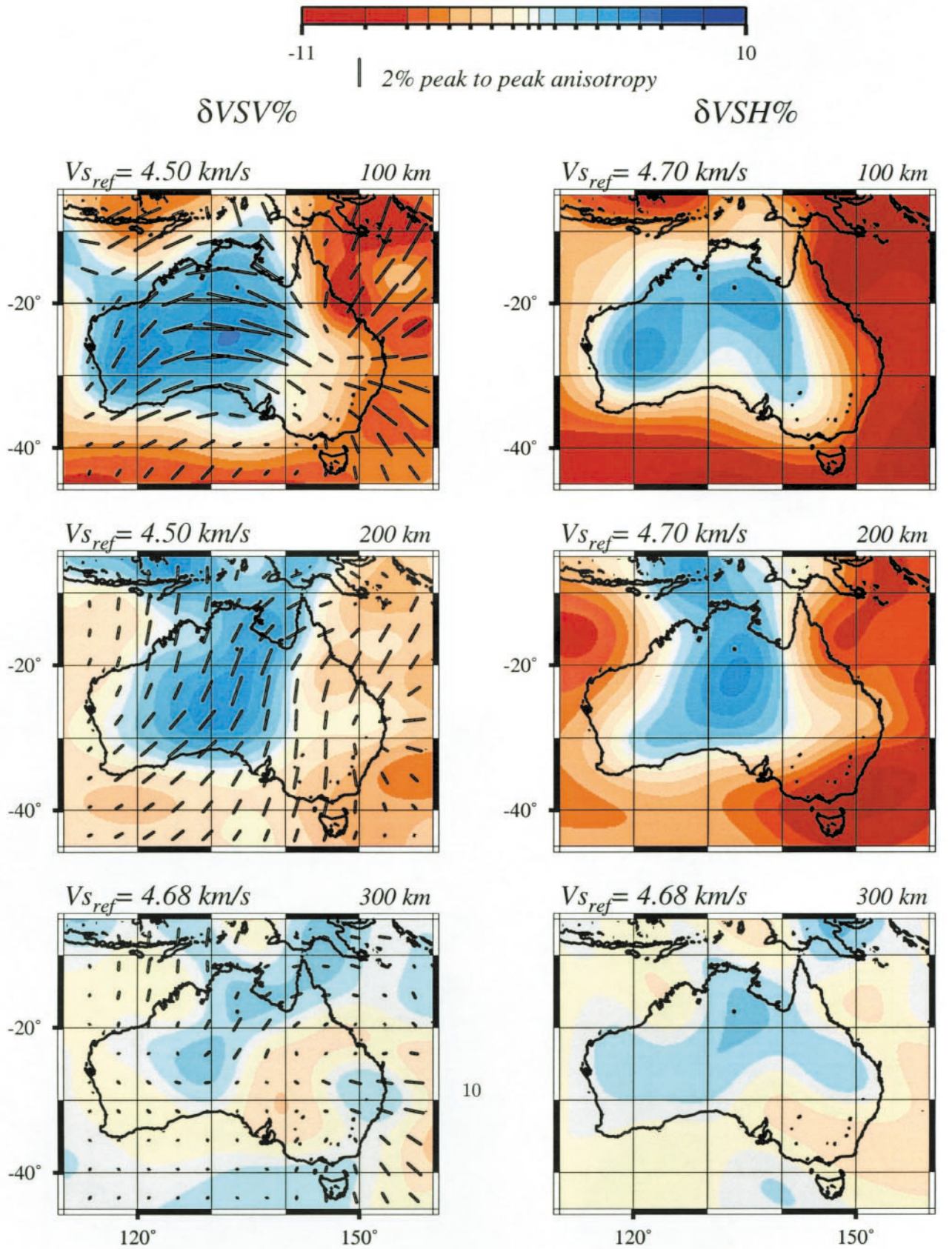

Figure 10 Left, SV wave heterogeneities and azimuthal anisotropy; right, SH wave heterogeneities. Tones represent velocity contrasts and bars display azimuthal anisotropy, the length of the bars indicating the strength of anisotropy. Note that the reference velocity used for SH is about 4% higher in the uppermost 200 km only.

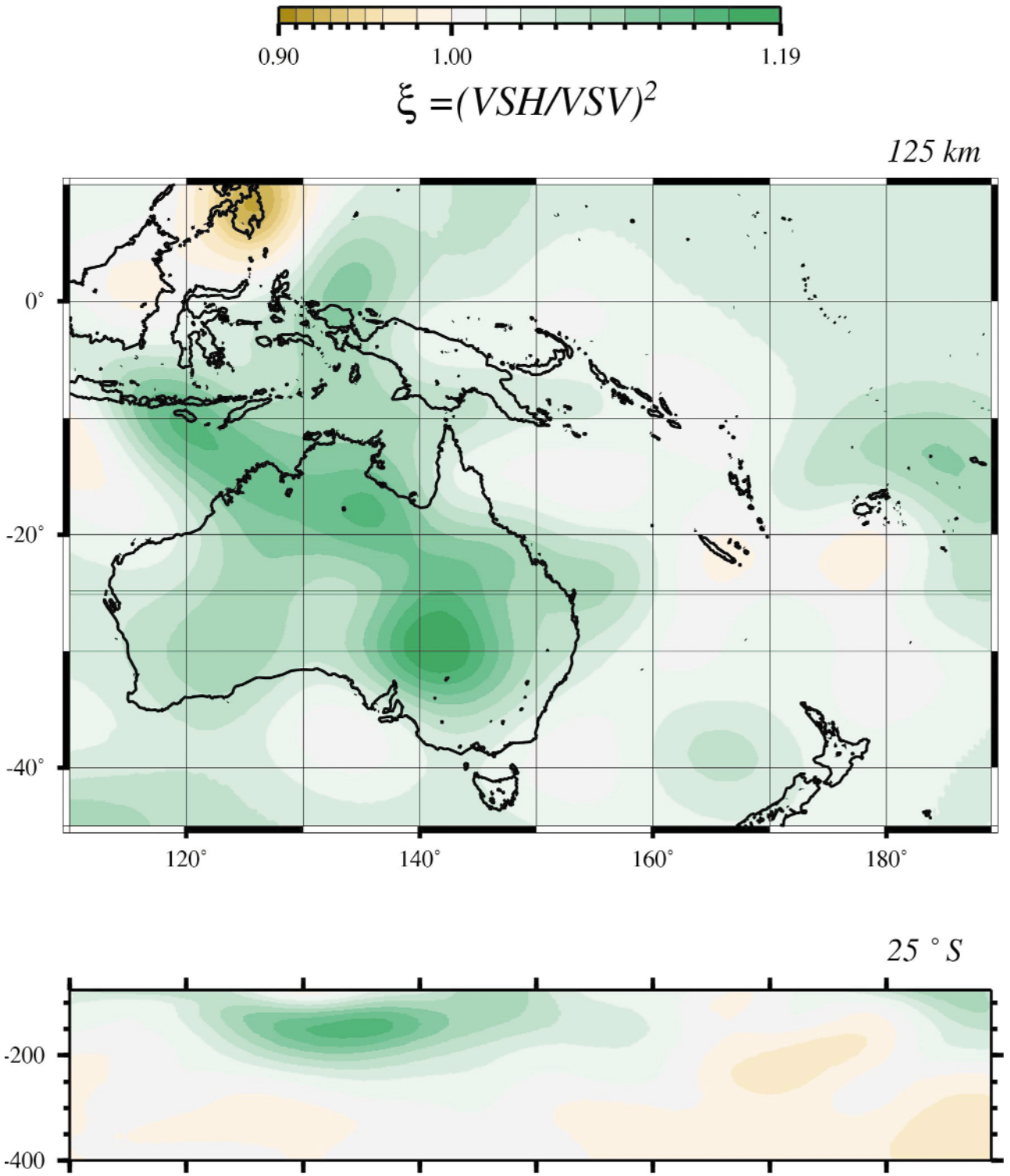

Figure 11 Polarisation anisotropy model at 125 km depth with a vertical cross-section at 25°S. SH waves have been found to propagate significantly faster than SV waves in the uppermost 200–250 km of the mantle for most of Australia.

[$\xi=(V_{sh}/V_{sv})^2$] is plotted. Values of ξ up to 1.19 (9% of polarisation anisotropy) have been obtained at 150 km for eastern Australia. This locally large anisotropy is difficult to reconcile with current mineralogical models and Debayle and Kennett (2000b) invoked the presence of strong lateral heterogeneities along the path and/or the effects introduced by the simplifying assumption of transverse isotropy in the starting Preliminary Reference Earth Model (PREM: Dziewonski & Anderson 1981) to explain the discrepancy. The amplitude of polarisation anisotropy, therefore, may not be determined accurately, but there is evidence (Lévêque & Cara 1985; Gaherty & Jordan 1995) which suggests that the location of polarisation anisotropy is correctly retrieved at depths within the current assumptions.

Figure 11 shows that, for Australia, significant polarisation anisotropy with SH faster than SV is present down to 200–250 km, in good agreement with the 1-D model of Gaherty and Jordan (1995). At larger depths, Debayle and Kennett (2000b) concluded that the SH/SV differences fall below the measurement errors and so are not required by the data. This layer where SH is faster than SV would correspond to regions where horizontal flow dominates in the upper mantle and where significant azimuthal anisotropy is expected (see Montagner 1994). The results presented here suggest that this layer would be about 250 km thick beneath Australia and somewhat thinner (about 100–150 km thick) in the adjacent oceanic areas (Figures 4, 11).

WHAT HAVE WE LEARNED ABOUT SEISMIC ANISOTROPY BENEATH AUSTRALIA?

The different studies that have addressed the question of upper mantle anisotropy beneath Australia have employed different techniques involving both body and surface waves. These techniques have yielded different answers, suggesting that the extraction of reliable information on the deep anisotropic structure of Australia requires a consideration of the limitations of each technique.

It is clear that the strongest limitation of classical SKS/SKKS analysis is lack of vertical resolution provided by the core shear phase; there is nothing in the surface observations to isolate the location of the anisotropy. Most of the previous splitting measurements of teleseismic shear waves beneath Australia have been based on the hypothesis that the anisotropic region can be approximated by a single homogeneous layer. Core shear phase-splitting measurements (mostly from SKS and SKKS) have been recently obtained by Clitheroe and van der Hilst (1998), who synthesised measurements from permanent and portable stations, and Ozalabey and Chen (1999), who revisited the data from the permanent stations across Australia. Both studies reached the conclusion of a weak or null splitting beneath Precambrian Australia. For the eastern Phanerozoic margin of the continent, significant splitting compatible with an upper mantle contribution to seismic anisotropy, has been observed by Clitheroe and van der Hilst (1998). The alignment of fast axis directions could either be explained by 'fossil' anisotropy frozen in the lithosphere (Silver & Chan 1991) or by present-day anisotropic flow (Vinnik *et al.* 1992).

Recently, Saltzer *et al.* (2000) have re-examined the validity of the assumption of a single homogeneous anisotropic layer when a vertically varying medium affects the shear-wave splitting. They observed a tendency of the measurements to mimic the anisotropy at the top part of the medium. In addition, for stronger heterogeneities, multiple scattering may produce a null result even for waves travelling in a strongly anisotropic medium. This may explain why no significant splitting has been observed beneath Precambrian Australia. Another possible explanation for central Australia is the presence of two anisotropic layers with orthogonal directions. If each layer produces a similar delay time between the fast and slow polarised wave, a resulting null splitting is expected for a vertically travelling wave which successively crosses the two layers.

More sophisticated analysis is thus needed to interpret shear-wave splitting results beneath Australia. Girardin and Farra (1999) used vertically travelling body waves converted at the different discontinuities to constrain the depth location of anisotropy beneath southeast Australia. They found a two-layered anisotropic model in the upper mantle beneath Canberra which would be in qualitative agreement with the surface-wave results presented here. For northern Australia Tong *et al.* (1994) used refracted shear waves returned from the transition zone and found a few percent of polarisation anisotropy in the upper mantle. They attributed this polarisation anisotropy to the depth interval between 210 and 410 km where a low Q has also been observed (Gudmundsson *et al.* 1994). A thinner asthenospheric layer located at the bottom of the cratonic lithosphere could also explain the observations but the dataset did not allow examination of the anisotropic properties of the lithosphere.

Horizontally propagating surface waves present the advantage of allowing the characterisation of seismic anisotropy as a function of depth, and until now the different studies for Australia have provided consistent results regarding the depth extent of polarisation anisotropy. Both the work by Gaherty and Jordan (1995) and the results presented here or in Debayle and Kennett (2000b) suggest that there is significant polarisation anisotropy down to 200–250 km depth within the Australian upper mantle. However, polarisation anisotropy results inferred from the discrepancy between Love and Rayleigh waves requires additional constraints on the anisotropic direction to allow unambiguous interpretation. Gaherty and Jordan (1995) used a dataset restricted to a single seismic corridor crossing Precambrian Australia, which did not allow them to extract any information regarding anisotropic directions. They interpreted their polarisation anisotropy measurements as reflecting a deformation mostly frozen in the continental lithosphere.

The simultaneous inversion of a large Rayleigh wave dataset with a good azimuthal ray coverage has ensured the extraction of the anisotropic directions as a function of depth, with a lateral resolution of a few hundred kilometres and a vertical resolution of a few tens of kilometres. This is sufficient to detect a change in the organisation of seismic anisotropy between the upper 150 km of the Earth and deeper mantle structure, which does not support the hypothesis of Gaherty and Jordan (1995) that the anisotropy is frozen throughout the lithosphere. A change of anisotropic properties with depth is also more easy to reconcile with indications from body waves for polarisation anisotropy in the asthenosphere (Tong *et al.* 1994) and with the observation of weak SKS splitting beneath Australia. If anisotropy was vertically coherent over a single lithospheric layer, significant SKS splitting would be expected.

However, we need to keep in mind that even with a fairly dense azimuthal distribution of rays our surface-wave analysis is based on a number of assumptions regarding the propagation of surface waves in anisotropic media. These limitations of the current theory restrict the frequency range and the number of modes for which surface waves can be safely processed, although the restrictions are relatively well known (Maupin 1989; Kennett 1995) and a careful analysis should allow us to obtain pertinent results on the

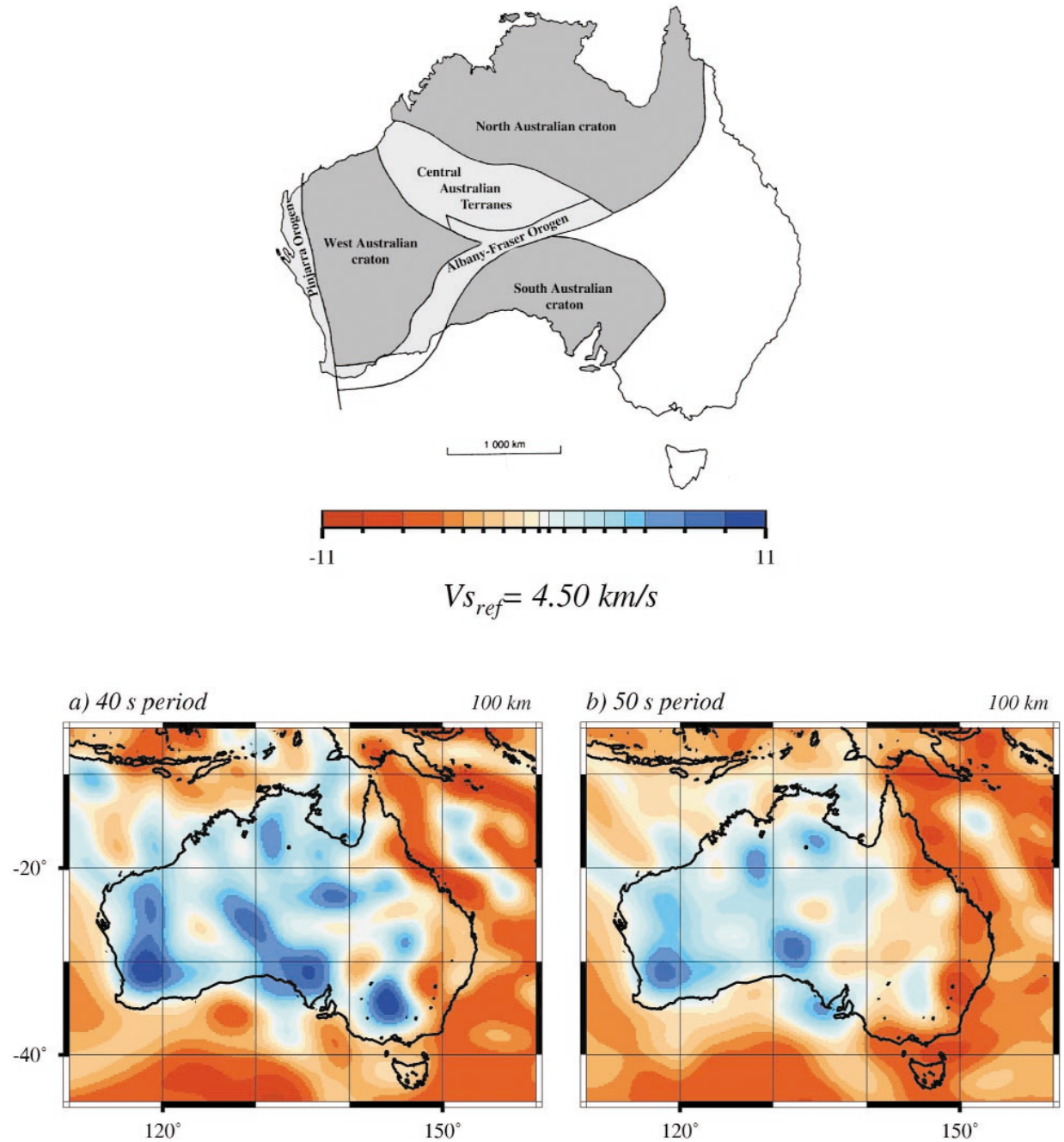

Figure 12 Top: the main Precambrian tectonic units of Australia (after Myers *et al.* 1996)—1830 Ma cratons; 1900–1300 Ma Central Australian Terranes; and the 1300 Ma Albany–Fraser Orogen. The Central Australian Terranes were accreted onto the North Australian Craton prior to its 1300 Ma suturing with the West and South Australian Cratons. Bottom: SV wave velocity pattern at 100 km depth derived from the Rayleigh wave inversion pushed to 40 s (a) or 50 s (b) period.

Earth's upper mantle. The horizontal resolution is limited to a few hundred kilometres and care needs to be taken with the interpretation of complex anisotropic patterns. Figure 9 shows that the horizontal smoothing may locally produce wrong anisotropic results in regions where the anisotropic directions change abruptly. In general, if the anisotropic directions in the upper layer of the mantle change with a scale-length smaller than the horizontal resolution, smoothing effects are likely to reproduce the complex pattern of anisotropy, but with directions that are locally wrong. In addition, we have shown in this paper that the short wavelength component of heterogeneity and anisotropy present in the upper layer of the model is affected by the cut-off frequency chosen when analysing the data. This is because shorter period surface waves are better for picking up the details of the shallow structures, but are also more likely to be affected by errors in the theory used for the analysis.

Choosing a reasonable cut-off frequency when analysing the data is difficult because it depends of the level of heterogeneity present in the actual Earth, which is one of the answers that we are trying to address in this class

of studies. To illustrate this difficulty, we present in Figure 12 a comparison between a reasonable *a priori* guess on the shape of the craton, derived from the work of Myers *et al.* (1996) and our S wave velocity maps from the 40 and 50 s inversions. A 40 s inversion seems to better underline the shape of the northern, southern and western Precambrian cratons. However, if the 40 s inversion provides a better horizontal resolution, it is also more likely to be sensitive to inaccuracy in the assumptions.

A good crosscheck of our results has recently been provided through an independent study of upper mantle anisotropy from electromagnetic data (Simpson 2001). The anisotropic directions obtained in this study are inferred to reflect the orientation of the fast a-axis of olivine crystals at depth greater than 150 km, so that they can be directly compared with our anisotropic maps. A good agreement between the electromagnetic strikes and our anisotropic map at 200 km depth has been observed (Simpson 2001) and suggests that despite the approximations underlying the methods, both techniques provide significant constraints on the Earth's upper mantle.

It is also reassuring to see that a closer correspondence with the results of Simons *et al.* (1999) can be obtained, at least for the upper 200 km of the mantle, by working in the same frequency range for the fundamental mode. This indicates that the differences which remain at 200 km depth and below are probably related to the treatment of higher mode information. It is likely that the strong level of heterogeneity present in the Australian upper mantle renders analysis of the higher modes dangerous at periods near 20 s, where problems related to the neglect of mode coupling and off-great-circle propagation are likely to become important.

CONCLUSIONS

The horizontal smoothing present in surface-wave inversion and the frequency dependence of the surface waves results obtained at 100 km depth for Australia suggest that the detail of the short wavelength variation in anisotropic directions should be interpreted with caution. However, the tomographic models are robust, especially when paths likely to experience complex propagation are removed. The application of the path-average approximation directly to the shear slowness is a reasonable approximation for current models of Australia. Surface waves clearly demonstrate that anisotropy is present down to 200–250 km depth beneath Australia with an organisation which is not coherent with depth. At least two anisotropic layers have been identified, the complex anisotropy in the uppermost layer being likely to reflect frozen deformation in the lithosphere. At depths greater than 150 km, the smoother anisotropic pattern with a dominant north–south component is more likely to reflect present-day deformation due to shearing at the bottom of the northward-moving Australian Plate. The depth of 150 km therefore marks an upper bound for the thickness of the 'mechanical' lithosphere, defined as the layer of the mantle that presents coherent horizontal motion. This is especially true for central Proterozoic Australia which is well sampled in the current surface-waves studies.

ACKNOWLEDGEMENTS

Part of this work was done while Brian Kennett was a visiting professor at University Louis Pasteur in Strasbourg. Our studies of the reliability of surface-wave images were stimulated by comments by Frederic Simons and Rob van der Hilst. Supercomputer facilities were provided by the French Institute for Development and Resources in Intensive Scientific Computing (IDRIS) and the Australian National University (ANU) in Canberra. The maps and the cross-section presented in this paper have been made using the GMT software (Wessel & Smith 1995). The IRIS and GEOSCOPE teams provided seismological data at the permanent and PASSCAL temporary stations. The management of the data from the portable experiments was made possible by the system established by Rob van der Hilst. Finally, special thanks are addressed to the Research School of Earth Sciences (ANU) personnel who collected the SKIPPY and KIMBA data in the field.

REFERENCES

Cara M. & Lévêque J. 1987. Waveform inversion using secondary observables. *Geophysical Research Letters* **14**, 1046–1049.

Clitheroe G. & van der Hilst R. D. 1998. Complex anisotropy in the Australian lithosphere from shear-wave splitting in broad-band SKS records. *In:* Braun J., Dooley J., Goleby B., van der Hilst R. & Klootwijk C. eds. *Structure and Evolution of the Australian Continent*, pp. 73–78. American Geophysical Union Geodynamics Monograph **26**.

Debayle E. 1999. SV-wave azimuthal anisotropy in the Australian upper-mantle: preliminary results from automated Rayleigh waveform inversion. *Geophysical Journal International* **137**, 747–754.

Debayle E. & Kennett B. L. N. 2000a. The Australian continental upper mantle: structure and deformation inferred from surface waves. *Journal of Geophysical Research* **105**, 25423–25450.

Debayle E. & Kennett B. L. N. 2000b. Anisotropy in the Australasian upper mantle from Love and Rayleigh waveform inversion. *Earth and Planetary Science Letters* **184**, 339–351.

Dziewonski A. M. & Anderson D. L. 1981. Preliminary reference Earth model. *Physics of the Earth and Planetary Interiors* **25**, 297–356.

Gaherty J. & Jordan T. H. 1995. Lehmann discontinuity as the base of anisotropic layer beneath continents. *Science* **268**, 1468–1471.

Girardin N. & Farra V. 1998. Azimuthal anisotropy in the upper mantle from observation of P-to-S converted phases: application to southeast Australia. *Geophysical Journal International* **133**, 615–629.

Gudmundsson O., Kennett B. L. N. & Goody A. 1994. Broadband observations of upper-mantle seismic phases in northern Australia and the attenuation structure in the upper mantle. *Physics of the Earth and Planetary Interiors* **84**, 207–226.

Kennett B. L. N. 1995. Approximations for surface-wave propagation in laterally varying media. *Geophysical Journal International* **122**, 470–478.

Kennett B. L. N. 1998. Guided waves in 3-dimensional structures. *Geophysical Journal International* **133**, 159–174.

Kennett B. L. N. 2003. Seismic structure in the mantle beneath Australia. *Geological Society of Australia Special Publicatin* **22** and *Geological Society of America Special Paper* **372**, 7–23.

Kennett B. L. N. & Yoshizawa K. 2002. A reappraisal of regional surface wave tomography. *Geophysical Journal International* **150**, 37–44.

Lévêque J. & Cara M. 1985. Inversion of multimode surface wave data: evidence for sub-lithospheric anisotropy. *Geophysical Journal of the Royal Astronomical Society* **83**, 753–773.

Lévêque J., Debayle E. & Maupin V. 1998. Anisotropy in the Indian Ocean upper mantle from Rayleigh- and Love-waveform inversion. *Geophysical Journal International* **133**, 529–540.

Maupin V. 1989. Surface waves in weakly anisotropic structures: on

the use of ordinary or quasi-degenerate perturbation methods. *Geophysical Journal International* **98**, 553–563.

Marquering H., Snieder R. & Nolet G. 1996. Waveform inversion and the significance of surface-wave mode coupling. *Geophysical Journal International* **124**, 258–278.

McEvilly T. 1964. Central US crust upper-mantle structure from Love and Rayleigh wave phase velocity inversion. *Bulletin of the Seismological Society of America* **54**, 1997–2016.

Montagner J. 1986. Regional three-dimensional structures using long-period surface waves. *Annales Geophysicae* **4**, 283–294.

Montagner J. 1994. Can seismology tell us anything about convection in the mantle? *Review of Geophysics* **32**, 115–137.

Montagner J. & Nataf H. C. 1986. A simple method for inverting the azimuthal anisotropy of surface waves. *Journal of Geophysical Research* **91**, 511–520.

Myers J., Shaw R. & Tyler I. 1996. Tectonic evolution of Proterozoic Australia. *Tectonics* **15**, 1431–1446.

Nataf H. C. & Ricard Y. 1995. 3SMAC: an a priori tomographic model of the upper mantle based on geophysical modelling. *Physics of the Earth and Planetary Interiors* **95**, 101–122.

Nolet G. 1990. Partitioned waveform inversion and two dimensional structure under the network of autonomously recording seismographs. *Journal of Geophysical Research* **95**, 8499–8512.

Ozalaybey S. & Chen W-P. 1999. Frequency dependent analysis of SKS/SKKS waveforms observed in Australia: evidence for null birefringence. *Physics of the Earth and Planetary Interiors* **114**, 197–210.

Saltzer R., Gaherty J. & Jordan T. H. 2000. How are vertical shear wave splitting measurements affected by variations in the orientation of azimuthal anisotropy with depth? *Geophysical Journal International* **141**, 374–390.

Silver P. & Chan W. 1991. Shear wave splitting and subcontinental mantle deformation. *Journal of Geophysical Research* **141**, 16429–16454.

Simons F., Zielhuis A. & van der Hilst R. D. 1999. The deep structure of the Australian continent from surface wave tomography. *Lithos* **48**, 17–43.

Simpson F. 2001. Resistance to mantle flow inferred from the electromagnetic strike of the Australian upper mantle. *Nature* **412**, 632–635.

Smith M. & Dahlen F. 1973. The azimuthal dependence of Love and Rayleigh wave propagation in a slightly anisotropic medium. *Journal of Geophysical Research* **78**, 3321–3333.

Tong C., Gudmundsson O. & Kennett B. 1994. Shear wave splitting in refracted waves returned from the upper mantle transition zone beneath northern Australia. *Journal of Geophysical Research* **99**, 15783–15797.

van der Hilst R., Kennett B., Christie D. & Grant J. 1994. Skippy: mobile broad-band arrays to study the seismic structure of the lithosphere and mantle beneath Australia. *EOS* **75**, 177–181.

van der Hilst R. D., Kennett B. L. N. & SHibutani T. 1998. Upper mantle structure beneath Australia from portable array deployments. *In:* Braun J., Dooley J., Goleby B., van der Hilst R. & Klootwijk C. eds. *Structure and Evolution of the Australian Continent*, pp. 39–58. American Geophysical Union Geodynamics Monograph **26**.

Vinnik L., Makeyeva L., Milev A. & Usenko A. Y. 1992. Global patterns of azimuthal anisotropy and deformations in the continental mantle. *Geophysical Journal International* **111**, 433–447.

Wessel P. & Smith W. H. F. 1995. New version of the Generic Mapping Tools released. *EOS* **76**, 329.

Woodhouse J. H. 1974. Surface waves in a laterally varying layered structure. *Geophysical Journal of the Royal Astronomical Society* **37**, 461–490.

Yoshizawa K. & Kennett B. L. N. 2002. Determination of the influence zone for surface wave paths. *Geophysical Journal International* **149**, 440–453.

Zielhuis A. & Nolet G. 1994. Shear-wave velocity variations in the upper mantle beneath central Europe. *Geophysical Journal International* **117**, 695–715.

Zielhuis A. & van der Hilst R. D. 1996. Upper-mantle shear velocity beneath eastern Australia from inversion of waveforms from Skippy portable arrays. *Geophysical Journal International* **127**, 1–16.

Received 4 July 2001; accepted 8 January 2002